Tuning the Electrical and Optical Properties of Graphene by Ozone Treatment for Patterning Monolithic Transparent Electrodes

Jiangtan Yuan,[†] Lai-Peng Ma,[†] Songfeng Pei, Jinhong Du, Yang Su, Wencai Ren, and Hui-Ming Cheng*

Shenyang National Laboratory for Materials Science, Institute of Metal Research, Chinese Academy of Sciences, Shenyang 110016, People's Republic of China.
[†]These authors contributed equally to this work.

ABSTRACT Tunable electrical and optical properties of graphene are vital to promote its use as film electrodes in a variety of devices. We developed an etching-free ozone treatment method to continuously tune the electrical resistance and optical transmittance of graphene films by simply varying the time and temperature of graphene exposure to ozone. Initially, ozone exposure dramatically decreases the electrical resistance of graphene films by p-doping, but this is followed by increases in the resistance and optical transmittance as a result of surface oxidation. The rate of resistance increase can be significantly increased by raising the treatment temperature. The ozone-oxidized graphene is not removed but is gradually transformed to graphene oxide (GO). On the basis of such effects of ozone treatment, we demonstrate a well-defined graphene pattern by using ozone photolithography, in which the ozone-treated graphene electrodes are monolithic but separated by insulating GO regions. Such a monolithic graphene pattern shows low optical contrast, a clean and more hydrophilic surface, indicating the promising use of ozone treatment to achieve high-performance graphene-based optoelectronic devices.

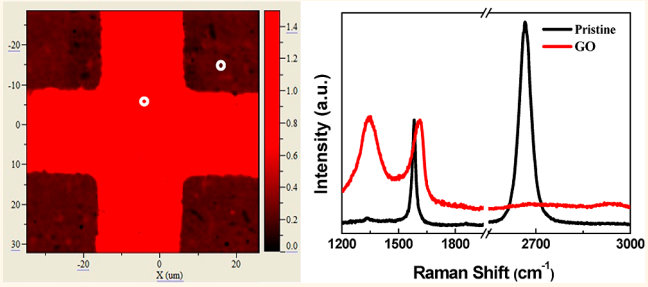

KEYWORDS: graphene · electrical conductivity · ozone treatment · pattern · transparent conductive film

Since its experimental isolation in 2004,[1] graphene has attracted tremendous attention due to its potentially wide applications. In particular, it holds great promise as a film electrode for various devices, as it possesses high electrical conductivity, transparency, flexibility, and stability against chemical environments.[2,3] However, the requirements for electrical conductivity (or sheet resistance) and optical transmittance vary significantly for different devices. For example, a combination of low electrical sheet resistance and high transparency is essential for high-performance transparent electrodes of display devices, solar cells, and smart windows, *etc.*[4−6] A typical strategy to achieve these properties is to dope a high-quality graphene film.[4] For electrodes in graphene sensors, a higher resistance can be acceptable since a functionalized surface with particular selectivity is preferred.[7−9] In addition, patterned electrodes are typically used in these devices.[10,11] Insulated graphene is required to fabricate a monolithic graphene pattern that separates highly conductive graphene electrodes with insulating regions. Compared with the etching-based patterning method, a monolithic pattern has a distinct advantage in avoiding the formation of edges and then the contamination of the photoresist residue at highly reactive graphene edges.[12−14] Therefore, it is highly desirable to develop a simple and effective strategy to tune the electrical and optical properties of graphene, which not only allows improvement in device performance but also expands its areas of application.[15,16]

Surface functionalization has shown great potential in tuning the electrical and optical properties of graphene. The transition of graphene from a conductor to a semiconductor

* Address correspondence to cheng@imr.ac.cn.

Received for review February 8, 2013 and accepted April 4, 2013.

Published online April 04, 2013
10.1021/nn400682u

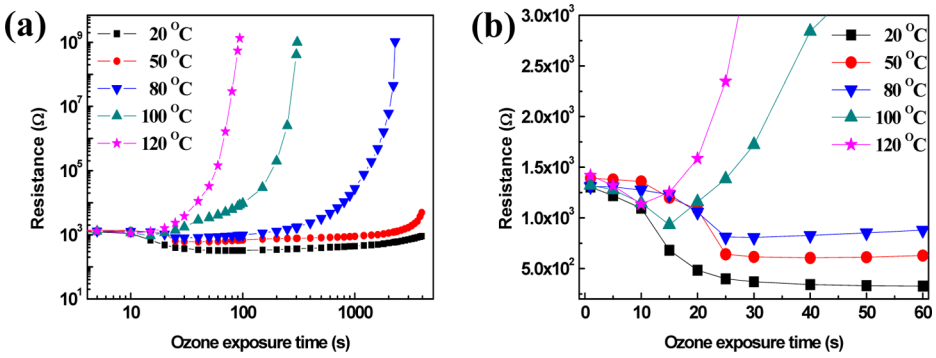

Figure 1. (a) Electrical resistance change of CVD-grown graphene films over time at different ozone treatment temperatures. (b) Resistance drop in the initial stage of ozone exposure.

and even an insulator has been reported,[17−20] and its optical transmittance and surface chemistry can be modified simultaneously. Surface oxidation is of particular interest since it is a relatively simple and low-cost process compared with other methods involving the use of fluorine- and chlorine-containing reagents.[18−20] Solution-based oxidation, such as the modified Hummers method, has been widely used for the synthesis of graphene oxide (GO),[21−23] and reducing GO to different extents has been useful in producing optoelectronic devices.[24] However, such a method suffers from the disruption of the graphene plane by strong oxidizing agents, the difficulty in achieving a homogeneous oxidation reaction for large-area films, and the inevitable contamination by sulfur- and/or nitrogen-containing groups. Alternatively, a gas-phase process has demonstrated its excellent control over the oxidation of graphene in the absence of contamination.[25] Of particular interest, theoretical calculation suggests that ozone treatment enables a tunable transition from metal to an Anderson insulator for graphene by grafting epoxide groups onto its plane.[26] It is also demonstrated that ozone oxidation can be used as a simple, scalable, and environment-friendly method to pattern carbon nanotube films.[27] Therefore, ozone treatment holds significant promise to tune the electrical conductivity of graphene by controllable oxidation. Up to now, however, the desirable metal−insulator transition arising from controllable ozone oxidation without etching the graphene plane has not been experimentally realized. The experimentally observed resistance increase of graphene was usually attributed to structural damage (*e.g.*, the formation of holes or trenches).[28,29] Moreover, the effect of ozone treatment on the electrical conductivity and structure of graphene is not well understood and needs to be further clarified. For example, both Raman investigations and field-effect transistor transport measurements have demonstrated the appreciable doping of graphene from short ozone exposure, but the expected resistance drop by doping was not obtained.[28,30,31] In addition, the effect of ozone treatment on the optical properties of graphene has not been reported.

In this study, we developed an etching-free ozone treatment method to tune the electrical resistance and optical transmittance of a monolayer chemical vapor deposition (CVD)-grown graphene film by controlling the time and temperature of its exposure to ozone. The results show that short ozone exposure significantly decreases its electrical sheet resistance by p-doping, whereas prolonged exposure progressively increases the resistance and the optical transmittance as a result of an oxidation reaction. The rate of electrical resistance increase can be significantly increased by raising the treatment temperature. The ozone-treated graphene is not removed but gradually transforms to GO. We demonstrate that the capability of ozone treatment to tune its electrical and optical properties can be used to fabricate a monolithic graphene pattern, which yields a well-defined graphene film electrode with low sheet resistance, low optical contrast, and a clean and more hydrophilic surface.

RESULTS AND DISCUSSION

In this work, we developed a mild ozone flow method to perform ozone treatment on graphene films. We first investigated the effect of ozone treatment on the electrical resistance of graphene films by *in situ* monitoring its change over time at different temperatures. The measurement was performed using a two-probe configuration on CVD-grown graphene films transferred onto a SiO_2/Si substrate. More details are provided in the Experimental Section. As shown in Figure 1a,b, at all investigated temperatures, there are clearly two regimes of resistance change: an initial resistance drop followed by a progressive resistance increase. Initially, a notable drop in resistance can be observed at temperatures below 80 °C. At 20 °C, 60 s exposure results in a significant drop of resistance by 75%, from ∼1300 to ∼320 Ω. The drop in resistance becomes lower as the temperature is increased. For 50, 80, 100, and 120 °C treatment, the initial resistance drops are 41, 38, 29, and 19%, respectively. This decrease is believed to be related to a competition between a doping effect and the oxidation of graphene, as discussed later. In the second stage, a

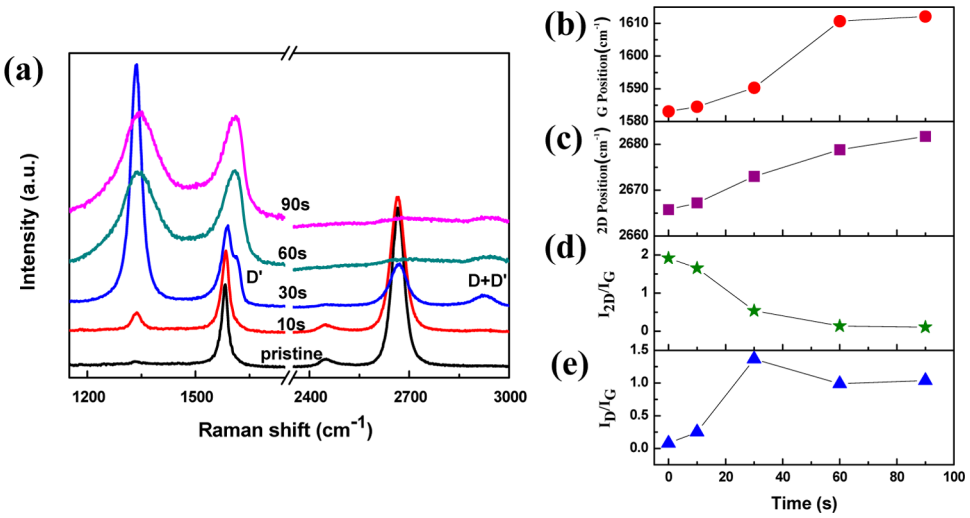

Figure 2. (a) Raman spectra change of the CVD-grown graphene films over time upon exposure to ozone at 120 °C; change of (b) G peak position and (c) 2D peak position, and the ratio of (d) I_{2D}/I_G and (e) I_D/I_G with time.

progressive increase in resistance is observed with increasing treatment time, and the rate of increase is highly dependent on the treatment temperature. At 20 °C, the resistance shows a slow increase to ~900 Ω by increasing the treatment time to ~4000 s, which is still lower than the initial value of ~1300 Ω. Treatment at 50 °C for the same time (4000 s) leads to a larger resistance of 4 kΩ. Above 80 °C, the resistance increases at a faster rate. Compared with the initial ~1.3 kΩ value, the resistance increases 6 orders of magnitude to around 1 GΩ, an insulating state, after 2000 s treatment at 80 °C. When the temperature is increased to 100 °C, the increase in resistance becomes even larger. Within about 400 s, the resistance is on the order of GΩ, and it only takes 90 s to produce insulating graphene by increasing the temperature to 120 °C. We did not examine the effect at temperatures higher than 120 °C because a lower temperature is favorable for the process of flexible electrode materials. *In situ* electrical measurements show that, by controlling the temperature and the time of ozone exposure, graphene can be continuously changed from a conductor to an insulator in a simple and efficient way.

To understand the mechanism of resistance change, we used Raman spectroscopy to investigate structure changes in graphene treated at 120 °C as a function of ozone exposure time (Figure 2). For the pristine sample, the negligible D peak at ~1340 cm^{-1} is a feature of the high quality of CVD-grown graphene films. As shown in Figure 2b–d, the positions of both the G and 2D peaks shift to a higher frequency and the intensity ratio of the 2D to the G peak (I_{2D}/I_G) decreases with time. In particular, 10 s ozone treatment leads to an upshift of ~1 cm^{-1} for both peaks. Alzina *et al.*[31] investigated the effect of ozone treatment on exfoliated graphene by Raman spectroscopy and found that a short exposure to ozone could p-dope graphene on the basis of a blue shift of the G (~2 cm^{-1}) and 2D peaks (~1 cm^{-1}), as well as a decrease in 2D peak intensity. Our Raman peak shifts agree well with their results, suggesting that p-doping is responsible for the resistance drop in the initial stage, as observed in Figure 1. Meanwhile, as shown in Figure 2e, 10 s ozone exposure only causes a slight increase in the D to G peak intensity ratio (I_D/I_G), which indicates that little structural change occurs by doping. In general, the D peak is activated by local basal distortion with the formation of defect-like sp^3 bonds in carbon materials. Significant structural transformation of sp^2 to sp^3 bonds can be observed after 30 s ozone treatment since I_D/I_G increases dramatically from ~0 to a maximum of ~1.5 and then stabilizes at approximately 1. In addition, D′ (~1620 cm^{-1}) and D+D′ (~2940 cm^{-1}) peaks appear after 30 s treatment, followed by the merging of the D′ peak with the G peak and a significantly weakened D+D′ peak. Furthermore, the 2D peak is hardly detectable after 60 s treatment. Such characteristics have also been observed in the structural evolution of GO during liquid-phase oxidation,[32] suggesting that graphene gradually transforms to GO, and as a result, the material becomes insulating. Zhang *et al.*[28] attributed the significant increase in D peak intensity and accompanying resistance increase to the substantial etching of the graphene by intense ozone oxidation. The formation of holes has also been reported in ozone-treated graphene, most of which are located at steps and folds.[33]

To elucidate the effect of ozone exposure on the graphene, we used atomic force microscopy (AFM) to compare the morphology of the pristine graphene with that treated by ozone. In contrast to previous results,[33] the wrinkles, which have been reported to show relatively higher activity toward oxidation,[34] still remain after the insulation treatment by ozone

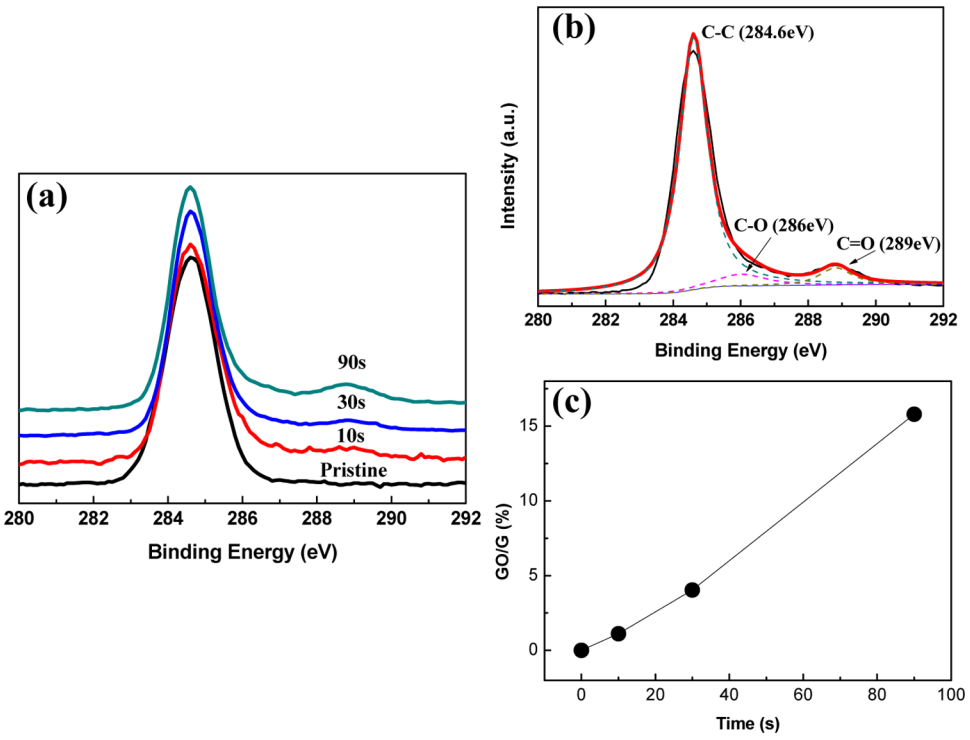

Figure 3. (a) XPS spectra changes of CVD-grown graphene films over time upon exposure to ozone at 120 °C. (b) Broad peak formed after 90 s ozone exposure can be fitted by two peaks, one at ~286 eV and the other at ~289 eV, which correspond to C−O and C═O bonds, respectively. (c) Ratio of oxygen-related carbon to sp^2 carbon (GO/G) estimated from the peak areas.

(Supporting Information Figure S1). The height profile further demonstrates that, after ozone treatment, the wrinkles have the same height (the left is ~6 nm, the right is ~4 nm) as that of pristine graphene. Additionally, no holes, trenches, or other detectable structural damage are observed in the graphene film. These results indicate that the observed change of graphene to an insulator results not from the etching and removal of graphene but from the significant oxidation reaction. We ascribe this etching-free process to the modification of the ozone treatment conditions as shown in the Experimental Section, which allows low-energy ozone molecules to react with graphene under relatively mild and controllable conditions.

To further confirm the oxidation of graphene by ozone, we performed X-ray photoelectron spectroscopy (XPS) measurements on the graphene films. In this case, we used graphene as-grown on Cu foils to eliminate the contamination of poly(methyl methacrylate) (PMMA) residue from the transfer process. As shown in Figure 3a, only the C1s peak can be observed at 284.6 eV prior to ozone exposure. Upon exposure to ozone for 10 s, a broad peak appears at 287−289 eV. Increasing the exposure time from 30 to 90 s increases its intensity remarkably. This broad peak can be fitted by two peaks, one at ~286 eV and the other at ~289 eV (Figure 3b), which correspond to C−O and C═O bonds, respectively.[35,36] The formation of C−O bonds indicates that oxygen-containing groups are formed upon exposure to ozone. By estimating the areas of the peaks due to C−C bonds and C−O bonds, we obtain the ratio of oxygen-bonded carbon to sp^2 carbon, denoted GO/G (Figure 3c). After 10 s exposure at 120 °C, which leads to the lowest resistance, GO/G is approximately 1.1%. Treatment for 30 s causes a relatively large increase in GO/G (to ~4%), suggesting that more oxygen-containing groups are formed on the graphene. After 90 s exposure, when the graphene becomes insulating, GO/G increases to 15%. These results are consistent with the Raman spectra and thus well explain the change of the electrical resistance. We also note that the GO/G for the insulating graphene produced by the ozone treatment is much lower than that produced by typical solution-based methods (~50%).[23,37] In fact, theoretical calculation suggests that graphene becomes insulating at a rather low epoxide density of 4%.[26] It is reasonable to believe that our process leads to more uniform oxidation of the graphene, thus producing insulating graphene at a much lower oxygen content.

Theoretical calculation suggests that the interaction between ozone and graphene involves two stages: the initial physisorption and the subsequent chemisorption (*i.e.*, the formation of oxygen-containing groups) of ozone molecules.[26] Jandhyala *et al.* found that the physisorbed ozone would lead to the upshift of the Dirac point, which is responsible for the p-doping of graphene.[38] An improved electrical conductivity (resistance drop) can then be expected with the increase of p-doping. In the subsequent chemisorption,

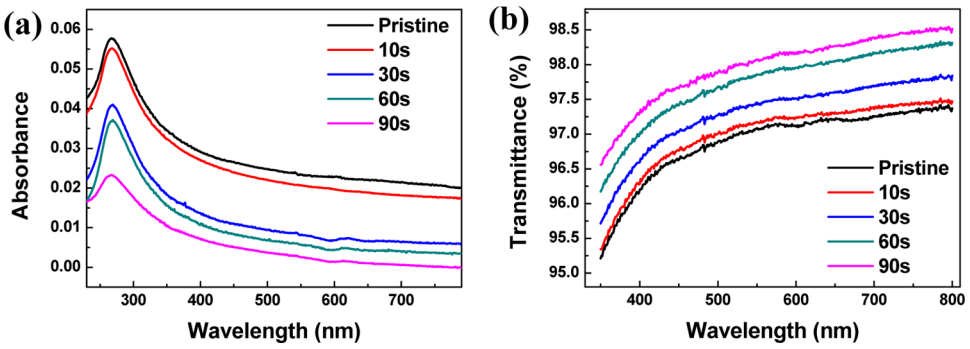

Figure 4. Changes in the (a) absorption and (b) optical transmittance spectra of CVD-grown graphene films with ozone exposure time at 120 °C.

however, no shift of the Dirac point is observed, and the epoxide groups act as defect scatters and decrease the electrical conductivity.[38] Consequently, graphene can be tuned from a conductor to an Anderson insulator by increasing the epoxide content.[26] These calculations are consistent with our experimental results, suggesting that the p-doping by physisorbed ozone should be primarily responsible for the resistance decrease of graphene during the initial ozone exposure, and the subsequent resistance increase is caused by the increase of oxygen-containing groups. In our experiment, we found that the resistance drops rapidly to the lowest point, followed by a slow resistance increase at 20 °C, which is consistent with the fact that ozone molecules readily physisorb on graphene. Because an energy barrier of 0.72 eV is required for the transition between physisorption and chemisorption,[38] the resistance change of graphene by physisorption is much faster than that by chemisorption. Another phenomenon is that the resistance drop becomes lower as the temperature is increased. This is because the physisorbed ozone molecules are easily desorbed from graphene with the increase of temperature. In addition, we found that the significant resistance drop obtained at 20 °C diminished within hours after ozone treatment. This result further confirms that the resistance drop was caused by physisorbed ozone, which is weakly attached to graphene and thus easily desorbed at ambient conditions. All of the above results can be well explained by the p-doping effect of physisorbed ozone. The physisorbed ozone can increase the hole concentration of graphene by p-doping; therefore, the resistance of graphene will decrease in the initial stage. We also note that a small amount of oxygen-containing groups form on the graphene upon exposure to ozone at 120 °C according to the XPS results in the initial ozone exposure (Figure 3), suggesting that chemisorption also existed. In fact, these two competing processes determine the resistance change by ozone treatment. In the initial stage, the physisorption is dominant and rapidly decreases the resistance of graphene, while in the second stage, the increasing chemisorption counteracts the effect of p-doping and increases the resistance of graphene.

It is worth noting that the widely used UV/ozone treatment, which directly exposes graphene to UV/ozone in the chamber, involves both ozone oxidation and bombardment of oxygen radicals.[28−31,33] The latter would cause structural damage of graphene and thus competes and even counteracts the doping effect of ozone in terms of the electrical conductivity. As a result, the expected resistance drop was not observed by using UV/ozone during the initial stage. In this work, the new ozone treatment process enables both the expected resistance drop of graphene by ozone doping and metal−insulator transition by ozone oxidation without etching its basal plane, providing a comprehensive description of the effect of ozone treatment on the electrical conductivity of graphene.

To verify the stability of the ozone-insulated graphene, we measured its resistance change with time at different temperatures. As observed in Figure S5, ozone-treated graphene is stable under ambient conditions. The stability of ozone-treated graphene over temperature and time paves the way for its potential applications as patterned monolithic electrodes.

The formation of C−O bonds alters not only the electrical resistance but also the optical transmittance of graphene as a result of the modified electronic structure. As shown in Figure 4a, a broad transition band centered at ~270 nm can be observed in the absorption spectra, which is a characteristic of graphene associated with the $\pi-\pi^*$ electron transition.[13,39] The band intensity shows a substantial decrease after 30 s ozone treatment, suggesting that the π electronic structure has been disrupted. From the viewpoint of electronic structure, the resistance increase caused by ozone treatment can be ascribed to the decreased mobility of electrons associated with the disrupted π structure in graphene. Correspondingly, the optical transmittance of graphene gradually increases with increasing ozone treatment time. As shown in Figure 4b, the transmittance increases from 97.1% for the pristine graphene to ~98.1% after 90 s ozone treatment, an increase of ~1%. The absorption

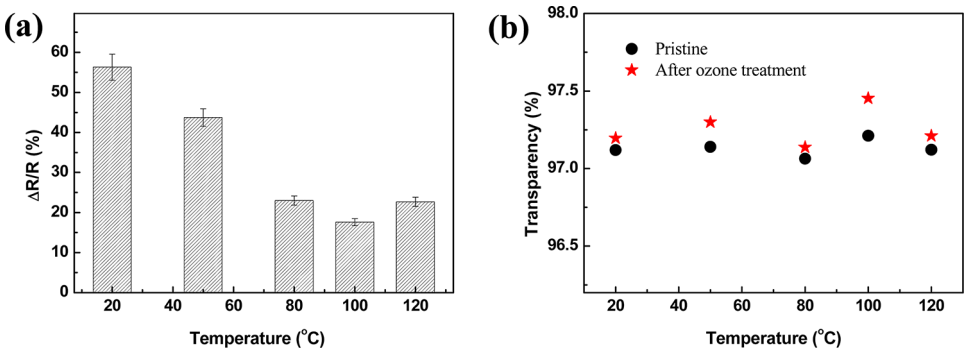

Figure 5. (a) Largest sheet resistance decrease of CVD-grown graphene films caused by oxygen doping at different temperatures. The times used for doping are 60 s (20 °C), 30 s (50 °C), 25 s (80 °C), 15 s (100 °C), and 10 s (120 °C). (b) Corresponding optical transmittance increase of the graphene films under identical treatment conditions.

and transmittance spectra are consistent with the gradual transition from graphene to GO. Note that the universal optical absorption of graphene still remains when graphene reaches the insulating state (*i.e.*, after 90 s treatment at 120 °C), suggesting that band gap is absent in the GO obtained. Such a gapless structure agrees well with the Anderson insulation of graphene by ozone oxidation.[26] The continuous and linear increase of transmittance also suggests that the transparency of graphene can be tuned by controlled ozone treatment.

On the basis of the above results, several advantages of using ozone can be inferred: (a) The electrical conductivity and the optical transmittance of graphene can be tuned by simply changing the temperature and time of ozone treatment. (b) The oxidized graphene is not removed but is well preserved. (c) As a gas oxidation process, it is free from contamination and is suitable to uniformly treat large-area graphene films. (d) It is cost-effective, scalable, and environment-friendly since ozone can be obtained directly from air. Moreover, (e) ozone treatment is superior to the conventional high-temperature gas-phase oxidation with regard to plastic substrates for flexible devices. The combination of these advantages makes ozone-treated graphene promising for use as film electrodes in various devices.

Of particular interest, ozone treatment shows great promise for achieving high-performance graphene transparent conducting electrodes that require a combination of low sheet resistance and high transparency. Figure 5a shows the largest decrease of sheet resistance of graphene films at different temperatures caused by the ozone doping effect (Figure S4). Notable decreases in sheet resistance can be observed at the temperatures investigated, which is consistent with the *in situ* two-probe test results. More significantly, ozone treatment at 20 °C leads to a 56.3% drop in the sheet resistance of a monolayer graphene film from 634 to 277 Ω/sq. This doping effect is comparable with all typical dopants reported,[4] and the resulting performance can satisfy the requirement of transparent electrodes in touch screens. A much lower sheet resistance can be expected by optimizing the transfer process, which is closely related to the high sheet resistance of pristine graphene. A distinct advantage of oxygen doping using ozone is that it will not decrease the transparency of graphene as do other doping reagents such as HNO_3 and $AuCl_3$.[40] In fact, oxygen doping using ozone leads to a slight increase of transparency by 0.1−0.3% at some temperatures, as shown in Figure 5b. This is favorable for high-performance graphene transparent electrodes. However, similar to other chemical doping agents, the resistance decrease caused by ozone treatment is also unstable with increasing storage time, and this needs to be improved.

Patterning of electrodes is an essential step in the fabrication of display devices and solar cells, *etc.* Extensive efforts have been devoted to developing suitable methods for patterning graphene films.[10,11,13,41] Benefitting from its compatibility with standard photolithography, plasma etching is the most used method in graphene patterning.[10] However, the etched graphene pattern suffers from an irregular edge geometry and contamination of the photoresist residue at highly reactive graphene edges.[13]

The etching-free ozone oxidation method developed allows us to avoid the above problems and to fabricate high-performance monolithic graphene patterns in combination with the standard photolithography. The patterning process by ozone photolithography developed in this work is illustrated in Figure S2. An as-grown CVD graphene film was first transferred to a target substrate (step a). The standard photolithography process was then used to obtain a patterned photoresist coating over the graphene film (step b).[42] Instead of plasma etching, the exposed region of graphene was changed to be insulating by the formation of GO by ozone oxidation (step c). After removing the photoresist coating, a monolithic graphene pattern was obtained in which conductive graphene electrodes are separated by insulating GO regions (step d), without the removal of any

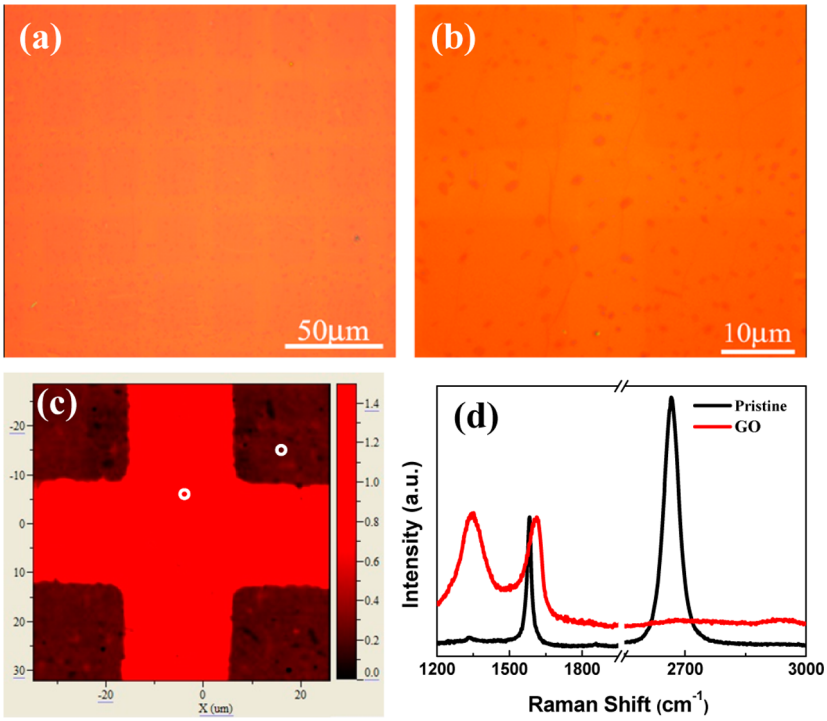

Figure 6. (a) Optical image of a graphene square pattern obtained by the ozone photolithography (steps a–d in Figure S2). (b) Enlarged part of (a). (c) Raman mapping (D/G) result corresponding to (b); the red cross represents the GO strips, and the black squares are the pristine graphene. (d) Raman spectra corresponding to the different regions in the pattern (white circles).

graphene. The sheet resistance of the graphene pattern obtained was further decreased by p-doping by additional room-temperature ozone treatment (step e). Figure 6a,b presents optical images of a graphene square pattern, in which the graphene squares and GO strips can be identified by the small optical contrast. The dark dots in Figure 6b are typical few-layer graphene islands grown on the Cu. A clear comparison can be seen by Raman mapping over the pattern, as shown in Figure 6c,d. The GO cross strips are characterized by a high D/G ratio, while the graphene squares show a negligible D/G ratio. We can also see that the oxidized region is uniform and has no holes or cracks, consistent with the AFM results, demonstrating a well-defined pattern with smooth edges.

Ozone photolithography avoids photoresist contamination at the graphene/GO boundary due to the monolithic pattern structure. As shown in Figure S3a,b, photoresist residue is clearly seen at the edges of graphene patterned by plasma photolithography. In contrast, such contamination is rarely detected in the ozone patterning. Moreover, this method has the advantage of a low optical contrast between the graphene and GO regions, which is crucial for high-performance graphene-based optoelectronic devices. Few-layer graphene transparent electrodes patterned by etching typically show high optical contrast; this may degrade the visual effect of display screens. For instance, a four-layer CVD graphene film shows a ~90% optical transmittance,[4,43] thus yielding a ~10% optical contrast between the areas in the electrode where graphene remains and where it has been removed. This value is reduced to 3.8% in a monolithic graphene pattern obtained by ozone photolithography, and this is more favorable for display applications (calculation details are shown in Supporting Information). In addition, for a transparent electrode used in optoelectronic devices such as solar cells and organic light-emitting diodes, a hydrophilic surface is highly desirable as it facilitates the deposition of a hole injection layer. However, the surface of pristine graphene is weakly hydrophilic.[44] We find that ozone photolithography is also effective in improving the wetting behavior of a graphene transparent electrode. Ozone photolithography reduces the contact angle from 70° for pristine graphene to 58° for a monolithic graphene pattern (Figure S3c,d). This is consistent with the fact that the formation of oxygen-containing groups on the graphene surface makes it more hydrophilic.

CONCLUSION

We achieved control over the electrical resistance and optical transmittance of CVD-grown graphene films by using etching-free ozone treatment. We found that in the first stage ozone exposure decreases the electrical sheet resistance of graphene by p-doping, while longer exposure in the second stage increases the resistance as a result of progressive oxidation to form GO. Ozone treatment leads to the complete

transition of graphene from a conductor to an insulator at temperatures above 80 °C without the removal of graphene. Meanwhile, the optical transmittance of the graphene films can be tuned. Taking advantage of the controllability and low temperature of a process that is free from contamination, a monolithic graphene pattern has been obtained by ozone photolithography, which combines low sheet resistance with a well-defined pattern, low optical contrast, a clean surface, and increased hydrophilicity, promising the wide use of ozone-treated graphene as film electrodes for various optoelectronic devices.

EXPERIMENTAL SECTION

Growth and Transfer of Graphene. Large-area graphene films were synthesized by CVD on copper foils. Typically, a 25 μm thick copper foil (Alfa Aesar, 99.8%) was annealed at 1000 °C for 30 min under a hydrogen flow and then exposed to a mixture of hydrogen and methane at a total pressure of 50 Pa for another 30 min before cooling to room temperature. For sample transfer, a thin layer of PMMA was deposited on the as-grown graphene/Cu foil. After etching away the Cu foil, the PMMA/graphene layer was rinsed with deionized water and then transferred to the target substrate (Si wafer capped with a 300 nm SiO_2 layer or quartz). Finally, the PMMA was carefully removed by acetone.

Ozone Treatment of Graphene Films. The ozone treatment was performed using an ozone generator (Guolin Industry Co., Ltd. Qingdao, China) with a hot plate (Xincheng Electronic Device Co., Ltd. Shenzhen, China). Instead of directly exposing graphene to ozone in the chamber, where the graphene would be exposed to high-energy ozone molecules, an ozone flow was used outside the chamber under ambient pressure, which was produced by flowing oxygen gas through the generator. This device allows us to control the oxidation extent by regulating the ozone flow rate and the reaction temperature. This configuration has the advantage that the size of the graphene films is not limited and can be easily scaled up. Graphene films were placed on a hot plate to investigate the influence of temperature on the whole oxidation process.

Characterization. The resistance change of graphene films over time at different ozone exposure temperatures was monitored with a two-probe configuration using a Keithley 2400 sourcemeter. Two copper wires were connected to the graphene film with silver paste, which produced good contact between them. The Raman spectra were acquired with a Jobin Yvon LabRAM HR800 Raman spectroscope at a laser wavelength of 532 nm. A 100× objective lens was used to focus the laser beam, and the spot size of the laser was ~1 μm^2. The laser power was set at ~272 μW to avoid damaging the graphene. The step size of Raman mapping is 500 nm. For the analysis of element composition, we used a XPS probe (ESCALAB 250) with a spot size of ~500 μm. In this case, as-grown graphene films on Cu foil were used to eliminate the contamination of PMMA residue from the transfer process. Absorption and transmittance spectra of graphene films on quartz under different conditions were recorded with a UV−vis−NIR spectrometer (Varian Cary 5000). The morphology of the graphene was characterized by AFM (Veeco MultiMode/Nano ScopeIIIa, operating in the tapping mode) and optical microscopy (Nikon ECLIPSE LV100).

Conflict of Interest: The authors declare no competing financial interest.

Acknowledgment. The authors sincerely thank Mr. Tianyuan Liu, Yang Gao, Wenbin Liu, and Dr. Feng Li for their help in the experiments. This work was supported by the National High-Tech Research and Development Program of China (No. 2012AA030303), Chinese Academy of Sciences (KGZD-EW-303-3), the National Natural Science Foundation of China (Nos. 50921004, 51102241, and 51102443).

Supporting Information Available: Additional information including AFM images before and after ozone treatment, the ozone patterning process, the clean surface, and the change of contact angle by ozone patterning. This material is available free of charge *via* the Internet at http://pubs.acs.org.

REFERENCES AND NOTES

1. Novoselov, K. S.; Geim, A. K.; Morozov, S. V.; Jiang, D.; Zhang, Y.; Dubonos, S. V.; Grigorieva, I. V.; Firsov, A. A. Electric Field Effect in Atomically Thin Carbon Films. *Science* **2004**, *306*, 666–669.
2. Geim, A. K.; Novoselov, K. S. The Rise of Graphene. *Nat. Mater.* **2007**, *6*, 183–191.
3. Geim, A. K. Graphene: Status and Prospects. *Science* **2009**, *324*, 1530–1534.
4. Bae, S.; Kim, H.; Lee, Y.; Xu, X.; Park, J. S.; Zheng, Y.; Balakrishnan, J.; Lei, T.; Kim, H. R.; Song, Y. I.; *et al.* Roll-to-Roll Production of 30-Inch Graphene Films for Transparent Electrodes. *Nat. Nanotechnol.* **2010**, *5*, 574–578.
5. Blake, P.; Brimicombe, P. D.; Nair, R. R.; Booth, T. J.; Jiang, D.; Schedin, F.; Ponomarenko, L. A.; Morozov, S. V.; Gleeson, H. F.; Hill, E. W.; *et al.* Graphene-Based Liquid Crystal Device. *Nano Lett.* **2008**, *8*, 1704–1708.
6. Wang, X.; Zhi, L.; Mullen, K. Transparent, Conductive Graphene Electrodes for Dye-Sensitized Solar Cells. *Nano Lett.* **2008**, *8*, 323–327.
7. Dong, X.; Shi, Y.; Huang, W.; Chen, P.; Li, L. J. Electrical Detection of DNA Hybridization with Single-Base Specificity Using Transistors Based on CVD-Grown Graphene Sheets. *Adv. Mater.* **2010**, *22*, 1649–1653.
8. Yavari, F.; Chen, Z.; Thomas, A. V.; Ren, W.; Cheng, H. M.; Koratkar, N. High Sensitivity Gas Detection Using a Macroscopic Three-Dimensional Graphene Foam Network. *Sci. Rep.* **2011**, *1*, 166.
9. Liu, Y.; Dong, X.; Chen, P. Biological and Chemical Sensors Based on Graphene Materials. *Chem. Soc. Rev.* **2012**, *41*, 2283–2307.
10. Pang, S. P.; Tsao, H. N.; Feng, X. L.; Mullen, K. Patterned Graphene Electrodes from Solution-Processed Graphite Oxide Films for Organic Field-Effect Transistors. *Adv. Mater.* **2009**, *21*, 3488–3491.
11. Dimiev, A.; Kosynkin, D. V.; Sinitskii, A.; Slesarev, A.; Sun, Z.; Tour, J. M. Layer-by-Layer Removal of Graphene for Device Patterning. *Science* **2011**, *331*, 1168–1172.
12. Wei, Z.; Wang, D.; Kim, S.; Kim, S. Y.; Hu, Y.; Yakes, M. K.; Laracuente, A. R.; Dai, Z.; Marder, S. R.; Berger, C.; *et al.* Nanoscale Tunable Reduction of Graphene Oxide for Graphene Electronics. *Science* **2010**, *328*, 1373–1376.
13. Zhang, L.; Diao, S.; Nie, Y.; Yan, K.; Liu, N.; Dai, B.; Xie, Q.; Reina, A.; Kong, J.; Liu, Z. Photocatalytic Patterning and Modification of Graphene. *J. Am. Chem. Soc.* **2011**, *133*, 2706–2713.
14. Lee, W. H.; Suk, J. W.; Chou, H.; Lee, J.; Hao, Y.; Wu, Y.; Piner, R.; Akinwande, D.; Kim, K. S.; Ruoff, R. S. Selective-Area Fluorination of Graphene with Fluoropolymer and Laser Irradiation. *Nano Lett.* **2012**, *12*, 2374–2378.
15. Bonaccorso, F.; Sun, Z.; Hasan, T.; Ferrari, A. C. Graphene Photonics and Optoelectronics. *Nat. Photonics* **2010**, *4*, 611–622.
16. Novoselov, K. S.; Fal'ko, V. I.; Colombo, L.; Gellert, P. R.; Schwab, M. G.; Kim, K. A Roadmap for Graphene. *Nature* **2012**, *490*, 192–200.
17. Elias, D. C.; Nair, R. R.; Mohiuddin, T. M.; Morozov, S. V.; Blake, P.; Halsall, M. P.; Ferrari, A. C.; Boukhvalov, D. W.; Katsnelson, M. I.; Geim, A. K.; *et al.* Control of Graphene's Properties by Reversible Hydrogenation: Evidence for Graphane. *Science* **2009**, *323*, 610–613.
18. Nair, R. R.; Ren, W.; Jalil, R.; Riaz, I.; Kravets, V. G.; Britnell, L.; Blake, P.; Schedin, F.; Mayorov, A. S.; Yuan, S.; *et al.* Fluorographene: A Two-Dimensional Counterpart of Teflon. *Small* **2010**, *6*, 2877–2884.

19. Robinson, J. T.; Burgess, J. S.; Junkermeier, C. E.; Badescu, S. C.; Reinecke, T. L.; Perkins, F. K.; Zalalutdniov, M. K.; Baldwin, J. W.; Culbertson, J. C.; Sheehan, P. E.; *et al.* Properties of Fluorinated Graphene Films. *Nano Lett.* **2010**, *10*, 3001–3005.
20. Wu, J.; Xie, L.; Li, Y.; Wang, H.; Ouyang, Y.; Guo, J.; Dai, H. Controlled Chlorine Plasma Reaction for Noninvasive Graphene Doping. *J. Am. Chem. Soc.* **2011**, *133*, 19668–19671.
21. Dikin, D. A.; Stankovich, S.; Zimney, E. J.; Piner, R. D.; Dommett, G. H.; Evmenenko, G.; Nguyen, S. T.; Ruoff, R. S. Preparation and Characterization of Graphene Oxide Paper. *Nature* **2007**, *448*, 457–460.
22. Park, S.; Ruoff, R. S. Chemical Methods for the Production of Graphenes. *Nat. Nanotechnol.* **2009**, *4*, 217–224.
23. Zhao, J.; Pei, S.; Ren, W.; Gao, L.; Cheng, H. M. Efficient Preparation of Large-Area Graphene Oxide Sheets for Transparent Conductive Films. *ACS Nano* **2010**, *4*, 5245–5252.
24. Loh, K. P.; Bao, Q.; Eda, G.; Chhowalla, M. Graphene Oxide as a Chemically Tunable Platform for Optical Applications. *Nat. Chem.* **2010**, *2*, 1015–1024.
25. Hossain, M. Z.; Johns, J. E.; Bevan, K. H.; Karmel, H. J.; Liang, Y. T.; Yoshimoto, S.; Mukai, K.; Koitaya, T.; Yoshinobu, J.; Kawai, M.; *et al.* Chemically Homogeneous and Thermally Reversible Oxidation of Epitaxial Graphene. *Nat. Chem.* **2012**, *4*, 305–309.
26. Leconte, N.; Moser, J.; Ordejon, P.; Tao, H.; Lherbier, A.; Bachtold, A.; Alsina, F.; Sotomayor Torres, C. M.; Charlier, J. C.; Roche, S. Damaging Graphene with Ozone Treatment: A Chemically Tunable Metal-Insulator Transition. *ACS Nano* **2010**, *4*, 4033–4038.
27. Su, Y.; Pei, S.; Du, J.; Liu, W.; Liu, C.; Cheng, H. Patterning Flexible Single-Walled Carbon Nanotube Thin Films by an Ozone Gas Exposure Method. *Carbon* **2013**, *53*, 4–10.
28. Zhang, E. X.; Newaz, A. K. M.; Wang, B.; Zhang, C. X.; Fleetwood, D. M.; Bolotin, K. I.; Schrimpf, R. D.; Pantelides, S. T.; Alles, M. L. Ozone-Exposure and Annealing Effects on Graphene-on-SiO_2 Transistors. *Appl. Phys. Lett.* **2012**, *101*, 121601.
29. Zhao, S.; Surwade, S. P.; Li, Z.; Liu, H. Photochemical Oxidation of CVD-Grown Single Layer Graphene. *Nanotechnology* **2012**, *23*, 355703.
30. Huh, S.; Park, J.; Kim, Y. S.; Kim, K. S.; Hong, B. H.; Nam, J. M. UV/Ozone-Oxidized Large-Scale Graphene Platform with Large Chemical Enhancement in Surface-Enhanced Raman Scattering. *ACS Nano* **2011**, *5*, 9799–9806.
31. Alzina, F.; Tao, H.; Moser, J.; Garcia, Y.; Bachtold, A.; Sotomayor-Torres, C. M. Probing the Electron−Phonon Coupling in Ozone-Doped Graphene by Raman Spectroscopy. *Phys. Rev. B* **2010**, *82*, 075422.
32. Wang, S. N.; Wang, R.; Liu, X. F.; Wang, X. W.; Zhang, D. D.; Guo, Y. J.; Qiu, X. H. Optical Spectroscopy Investigation of the Structural and Electrical Evolution of Controllably Oxidized Graphene by a Solution Method. *J. Phys. Chem. C* **2012**, *116*, 10702–10707.
33. Tao, H. H.; Moser, J.; Alzina, F.; Wang, Q.; Sotomayor-Torres, C. M. The Morphology of Graphene Sheets Treated in an Ozone Generator. *J. Phys. Chem. C* **2011**, *115*, 18257–18260.
34. Starodub, E.; Bartelt, N. C.; McCarty, K. F. Oxidation of Graphene on Metals. *J. Phys. Chem. C* **2010**, *114*, 5134–5140.
35. Pei, S. F.; Zhao, J. P.; Du, J. H.; Ren, W. C.; Cheng, H. M. Direct Reduction of Graphene Oxide Films into Highly Conductive and Flexible Graphene Films by Hydrohalic Acids. *Carbon* **2010**, *48*, 4466–4474.
36. Lee, B. K.; Park, S. Y.; Kim, H. C.; Cho, K.; Vogel, E. M.; Kim, M. J.; Wallace, R. M.; Kim, J. Y. Conformal Al_2O_3 Dielectric Layer Deposited by Atomic Layer Deposition for Graphene-Based Nanoelectronics. *Appl. Phys. Lett.* **2008**, *92*, 203102.
37. Eda, G.; Lin, Y. Y.; Mattevi, C.; Yamaguchi, H.; Chen, H. A.; Chen, I. S.; Chen, C. W.; Chhowalla, M. Blue Photoluminescence from Chemically Derived Graphene Oxide. *Adv. Mater.* **2010**, *22*, 505–509.
38. Jandhyala, S.; Mordi, G.; Lee, B.; Lee, G.; Floresca, C.; Cha, P.; Ahn, J.; Wallace, R. M.; Chabal, Y. J.; Kim, M. J.; *et al.* Atomic Layer Deposition of Dielectrics on Graphene Using Reversibly Physisorbed Ozone. *ACS Nano* **2012**, *6*, 2722–2730.
39. Li, D.; Muller, M. B.; Gilje, S.; Kaner, R. B.; Wallace, G. G. Processable Aqueous Dispersions of Graphene Nanosheets. *Nat. Nanotechnol.* **2008**, *3*, 101–105.
40. Gunes, F.; Shin, H. J.; Biswas, C.; Han, G. H.; Kim, E. S.; Chae, S. J.; Choi, J. Y.; Lee, Y. H. Layer-by-Layer Doping of Few-Layer Graphene Film. *ACS Nano* **2010**, *4*, 4595–4600.
41. Kim, T.; Kim, H.; Kwon, S. W.; Kim, Y.; Park, W. K.; Yoon, D. H.; Jang, A.-R.; Shin, H. S.; Suh, K. S.; Yang, W. S. Large-Scale Graphene Micropatterns *via* Self-Assembly-Mediated Process for Flexible Device Application. *Nano Lett.* **2012**, *12*, 743–748.
42. Su, Y.; Du, J.; Pei, S.; Liu, C.; Cheng, H. M. Contamination-Free and Damage-Free Patterning of Single-Walled Carbon Nanotube Transparent Conductive Films on Flexible Substrates. *Nanoscale* **2011**, *3*, 4571–4574.
43. Li, X. S.; Zhu, Y. W.; Cai, W. W.; Borysiak, M.; Han, B. Y.; Chen, D.; Piner, R. D.; Colombo, L.; Ruoff, R. S. Transfer of Large-Area Graphene Films for High-Performance Transparent Conductive Electrodes. *Nano Lett.* **2009**, *9*, 4359–4363.
44. Hecht, D. S.; Hu, L.; Irvin, G. Emerging Transparent Electrodes Based on Thin Films of Carbon Nanotubes, Graphene, and Metallic Nanostructures. *Adv. Mater.* **2011**, *23*, 1482–1513.